VIII International Conference on Computational Methods for Coupled Problems in Science and Engineering
COUPLED PROBLEMS 2019
E. Oñate, M. Papadrakakis and B. Schrefler (Eds)

COMPUTATIONAL MODELLING OF GAS FOCUSED THIN LIQUID SHEETS

GREGA BELŠAK[*], SAŠA BAJT[†] AND BOŽIDAR ŠARLER[*,]**

[*] Laboratory for Simulation of Materials and Processes
Institute of Metals and Technology
Lepi pot 11, SI-1000 Ljubljana, Slovenia
email: grega.belsak@imt.si

[†] Deutsches Elektronen-Synchrotron DESY
Notkestraße 85, 22607 Hamburg, Germany
email: sasa.bajt@desy.de

[**] Laboratory for Fluid Dynamics and Thermodynamics
Faculty of Mechanical Engineering University of Ljubljana
Aškerčeva 6, SI-1000 Ljubljana, Slovenia
email: bozidar.sarler@fs.uni-lj.si

Key words: Microfluidics, Liquid Sheets, Multiphase System, Surface Tension Driven Flow

Abstract. Formation of liquid sheets has been demonstrated as a critical capability needed in many different research fields. Many different types of liquid sheets have been produced experimentally, its thickness ranging from few tens of nanometres to few micrometres. Due to the small size of such systems, where physical parameters such as thickness, velocity and temperature are difficult to measure, a need for numerical simulation of liquid sheets arises. In this paper we demonstrate such capability with sheets that can be used in experiments with synchrotrons, X-ray free electron lasers or lab sources. A modified gas dynamic virtual nozzle (GDVN) design is used in order to generate micrometre thin sheets. The system is characterised by a strongly coupled problem between the focusing gas flow and the liquid sheet flow. Investigation of varying physical properties of liquid is performed in order to demonstrate the effects on the sheet production. It was found that the primary sheet thickness is not sensitive to the variation of liquid viscosity and density. On the other hand, the variation of surface tension greatly affects the thickness and the width of a primary sheet, such as expected in flows where surface tension is the dominating force. Findings demonstrate that by lowering the surface tension of a liquid, i.e. changing liquid from water to alcohol for example, would produce thinner and wider sheets. Simulations were produced with OpenFOAM, relying on finite volume based multiphase solver "compressibleInterFoam", capable of simulating free surfaces. Mixture formulation of a multiphase system consists of an incompressible liquid phase along with a compressible ideal gaseous phase. Such model was also used in axisymmetric GDVN micro-jet simulations preformed in our previous work. Due to the need for 3D simulations and huge computational resources needed, an adaptive approach was chosen. This made the simulations of liquid sheets of thicknesses down to 500 nm possible.

1 INTRODUCTION

Controlled multiphase fluid flows are being utilized in wide range of scientific research and industrial applications. Generally, these types of flows can be of a wide variety of length scales, ranging from the kilometre down to the nanometre size. In a microfluidics system where typical lengths are measured in few tens of micrometres, the dominant driving force tends to be the surface tension. These types of flows are called surface tension driven flows. Such flows have long been utilized experimentally, to produce droplets of ranging sizes, streams of varying diameters etc. The advances in numerical modelling and computational capabilities allow the exploration of these types of flows through simulations. One such application is the use of a gas dynamic virtual nozzle GDVN [1,2] which utilizes flow of a highly compressible gas through a nozzle throat to focus a stream of liquid into a micrometre size jet that eventually breaks up into droplets. Capability of simulating such systems was previously demonstrated [3]. In this paper a somewhat modified GDVN is employed that does not produce an axisymmetric jet, but rather a single stream of perpendicular liquid sheets [4,5]. The work presented here gives a computational insight into behaviour of such liquid sheet systems.

The structure of the paper is organized as follows: Section 2 illustrates the 3D model of the designed nozzle. Section 3 presents the governing equations, while section 4 describes the numerical methods used. The results of this study are shown in section 5. The paper concludes with the final remarks in section 6.

2 LIQUID SHEET NOZZLE

The liquid sheet nozzle design is loosely based on a nozzle design from Koralek et. al paper [4], which in turn was based on gas dynamic virtual nozzle (GDVN). Figure 1 depicts the nozzle.

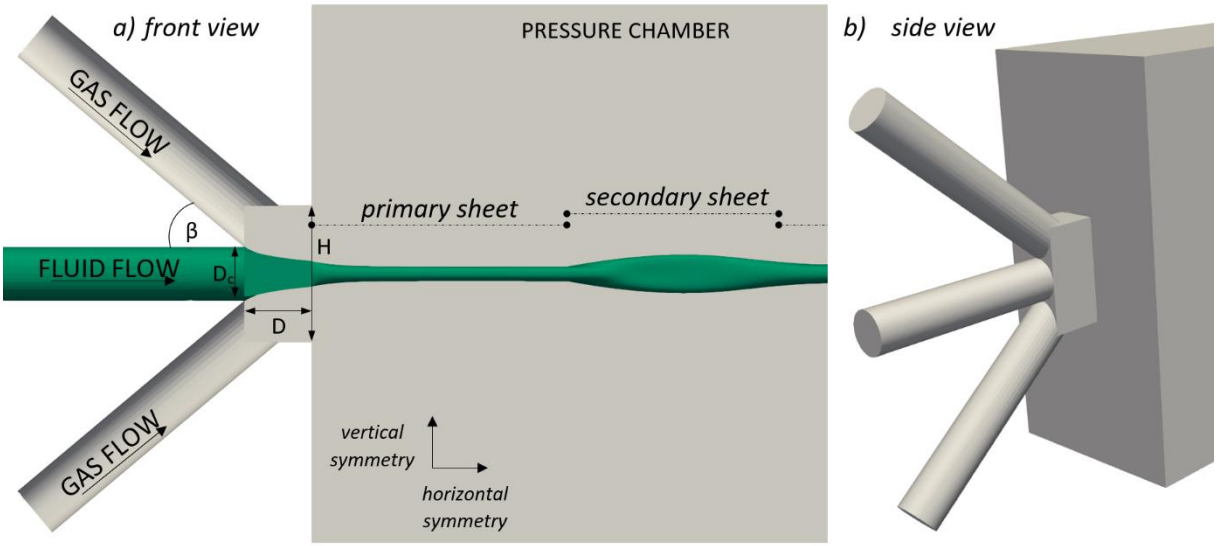

Figure 1: Graphical representation of the nozzle used in the production of liquid sheet viewed from two different directions: (a) front view, (b) side view.

It consists of a central capillary through which a liquid is delivered into the pressure chamber. Gas is injected trough two capillaries which are angled at $\beta = \pm 40°$ with respect to the central capillary. All three capillaries are chosen to be of the same diameter $D_c = 20$ μm. They converge in the nozzle throat of width $D = 25$ μm and height $H = 50$ μm. The nozzle throat forms a rectangular parallelepiped of dimensions (D, H, D_c).

3 GOVERNING EQUATIONS

In the present section a set of equations describing the multiphase fluid flow through the nozzle into a pressure chamber is presented. The physical model corresponds to a highly compressible Newtonian fluid in the laminar flow regime, described by the following set of mass (1), momentum (2) and energy conservation equations (3).

$$\frac{\partial \rho}{\partial t} + \nabla \cdot (\rho \boldsymbol{u}) = 0 \tag{1}$$

$$\frac{\partial \rho \boldsymbol{u}}{\partial t} + \nabla \cdot (\rho \boldsymbol{u}\boldsymbol{u}) = -\nabla p + \nabla \cdot (\mu [\nabla \boldsymbol{u}]) + \nabla \cdot (\mu [\nabla \boldsymbol{u}]^T) - \frac{2}{3}\nabla(\mu \nabla \cdot \boldsymbol{u}) + \boldsymbol{f}_{st} \tag{2}$$

$$\frac{\partial \rho c_v T}{\partial t} + \nabla \cdot (\rho c_v T \boldsymbol{u}) + \frac{\partial \rho \frac{1}{2} U^2}{\partial t} + \nabla \cdot (\rho \tfrac{1}{2} U^2 \boldsymbol{u}) + \nabla \cdot (p \boldsymbol{u}) = \nabla \cdot (k \nabla T) \tag{3}$$

Velocity, density, pressure, temperature, dynamic viscosity, specific heat, velocity magnitude and thermal conductivity are given by $\boldsymbol{u}, \rho, p, T, \mu, c_v, U$ and k. In dealings with a multiphase flow an ever present interface needs to be properly solved for. This is handled by an algebraic volume of fluid method, represented by the following two equations:

$$\frac{\partial \alpha}{\partial t} + \nabla \cdot (\alpha \boldsymbol{u}) + \nabla \cdot [(\alpha(1-\alpha)\boldsymbol{u}_c] = 0 \tag{4}$$

$$|\boldsymbol{u}_c| = \min[C_\alpha |\boldsymbol{u} \cdot \boldsymbol{n}|, |\boldsymbol{u} \cdot \boldsymbol{n}|] \tag{5}$$

α stands for a volumetric fraction of a liquid accompanied by the interfacial compression velocity $\boldsymbol{u}_c$, free compression parameter C_α and normal vector to the interface $\boldsymbol{n}$. Continuum surface force model [6] implements a surface tension force as a body force in the momentum equation by evaluating the curvature of the interface as:

$$\boldsymbol{f}_{st} = \sigma \kappa \nabla \alpha \tag{6}$$

$$\kappa = -\nabla \cdot \left(\frac{\nabla \alpha}{|\nabla \alpha|}\right) \tag{7}$$

where σ is surface tension and κ is the mean curvature of the interphase boundary.

4 NUMERICAL METHOD

The simulations in the present work are performed by an open source code OpenFOAM [7] - version 1806, which uses finite volume method alongside with the algebraic volume of fluid method. The nature of the nozzle flow requires the gas flow to be considered as compressible while the liquid flow is of constant density. The proper description of the interphase boundary dictates the choice of "compressibleInterFoam" solver. Non-axisymmetric nozzle design calls for a three dimensional model. A quarter symmetry of the liquid sheets is assumed, which reduces the number of cells by a factor of 4 in comparison to the full 3D simulation. Dynamic meshing capability is utilized to further reduce the calculation time. The refinement criterion is the position of the interface. This results in a basic mesh with 150 000 cells at the beginning of the simulation and 380 000 cells for a fully developed sheet. The interface cell resolution is set to 0.25 μm. Simulations were performed with PISO solver with a maximum Courant number set to 0.95. The simulations were run in parallel on 36 cores on HPC where each simulation took approximately one day to complete. They were run past the time when the sheet stabilized, which occurs at roughly 20 μs real time. Figure 2 depicts a cross-section through a sample mesh where the use of adaptive meshing can be observed clearly, along with an overlying developed sheet.

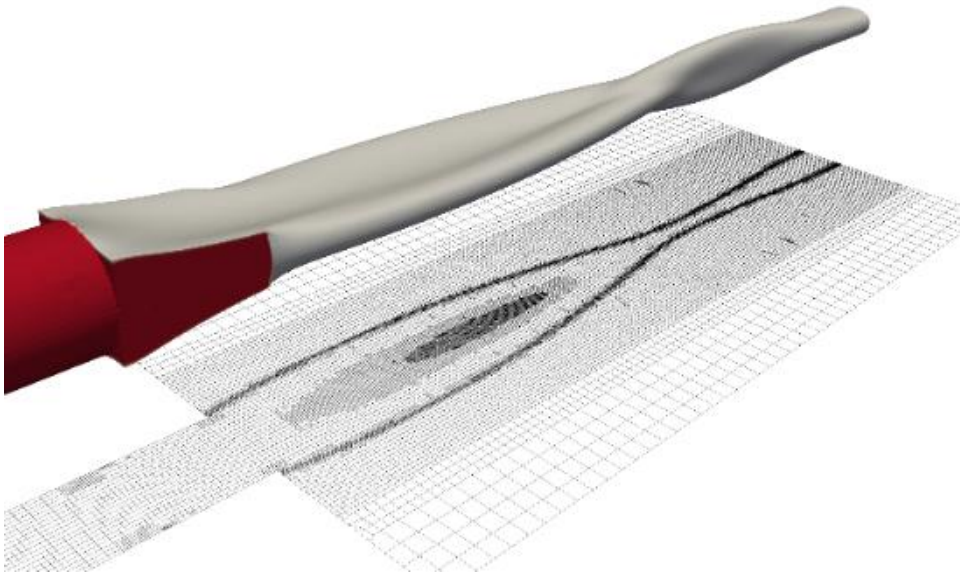

Figure 2: Scheme of a section of a mesh in a fully developed simulation. Darker regions with the mesh refinement can be observed. The minimum mesh resolution is 0.25 μm.

5 RESULTS

A desire, to know which liquid is most suitable to use for the production of microscopic sheets in the defined nozzle layout, led to the following set of simulations. Here three parametric studies were performed, where a wide range of liquid properties and its effects on the sheet shape were considered (see Table 1). The range was set in such a way that the two most commonly used liquids, water and ethanol, would fall under the investigation. Helium was used

as a focusing gas with pressure chamber gas pressure set to 1 bar. Gas and liquid flow rates were kept constant at 4 mg/min and 80 µL/min, respectively. Due to the microscopic size of the sheet the flow is surface tension driven. We have varied the density, viscosity and the surface tension in the simulations. The quality of the sheets could be evaluated using the number of the perpendicular sheet surfaces, their width, thickness, position relative to the nozzle exit, velocity or the stability of their length. The main criteria in the present study represents the minimization of the sheet thickness. The results are presented below.

Figures 3 to 5 show the vertical symmetry axis thickness of the primary sheet along the horizontal symmetry axis (Figure 1). It can be observed that the thickness of the sheet that emerges from the nozzle is initially 20 µm thick, corresponding to the liquid capillary diameter. The sheet is partially focused already inside the nozzle, shown on graphs left to the vertical black line, and additionally outside to a minimum thickness marked with a circle. The primary sheet then transitions to a perpendicular secondary sheet which can be seen in surface tension variation graphs but not in the density and viscosity graphs. Final results along with corresponding physical parameters are shown in Table 1. The secondary sheets are not investigated here. Figure 3 shows the effect of the density variation of the liquid on the sheet thickness. It is observed that the majority of the focusing happens inside the nozzle and the sheet thickness reaches its minimum roughly 6 µm from the nozzle exit. The 20 percent change in density has virtually no effect on the position of the minimum thickness sheet and only a slight decrease in thickness is observed with the decrease in density.

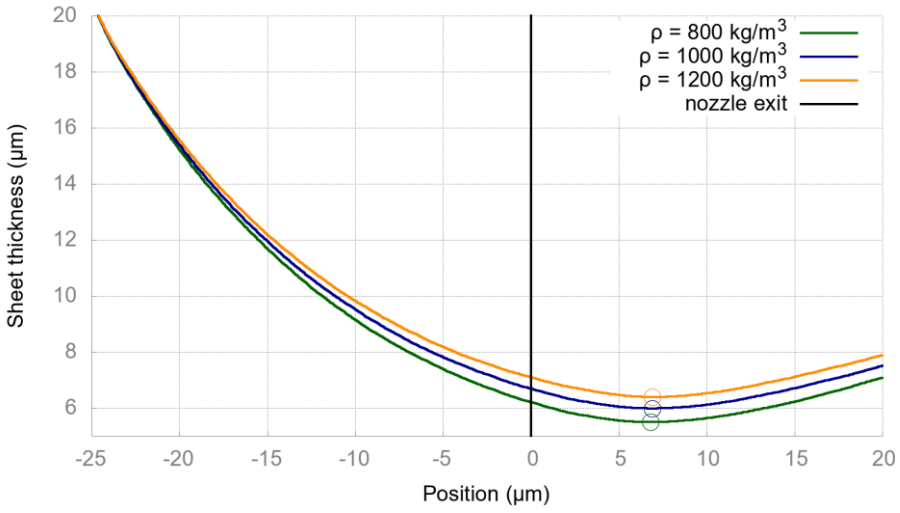

Figure 3: Thickness along the central region of the primary sheet for different liquid densities. The black line denotes the nozzle exit, while the circles represent the minimum achieved sheet thickness.

Figure 4 shows roughly 50 percent variation of the dynamic viscosity of the liquid on the sheet thickness. Similarly as in density, the position of minimum is practically unaffected. The thickness variation is observed to be less than in density study, despite using larger variations. This leads to the conclusion that the flow under these conditions is less sensitive to the liquid viscosity than it is to the liquid density.

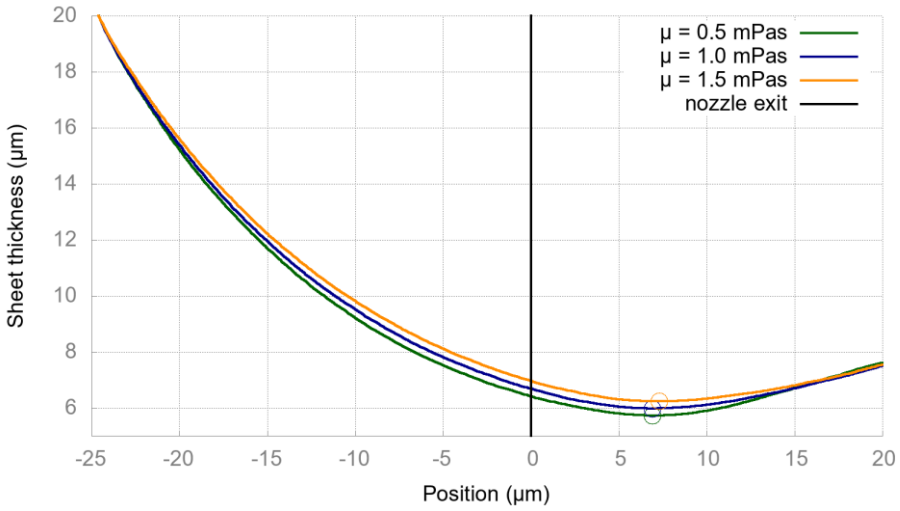

Figure 4: Thickness along the central region of the primary sheet for different liquid viscosity. The black line denotes the nozzle exit, while the circles represent the minimum achieved sheet thickness.

Lastly, we examine the effect of the surface tension variation, seen in Figure 5. The variations of the position of minimum thickness and thickness itself are quite substantial in this case. Changing the liquid with surface tension corresponding to water with one corresponding to ethanol results in a sheet thickness reduction from six micrometre thickness down to roughly a micrometre thickness. The simulation with even lower surface tension would thus require an even finer mesh resolution than used in the present work, since the sheet would become thinner and it would breakup due to too rough discretization.

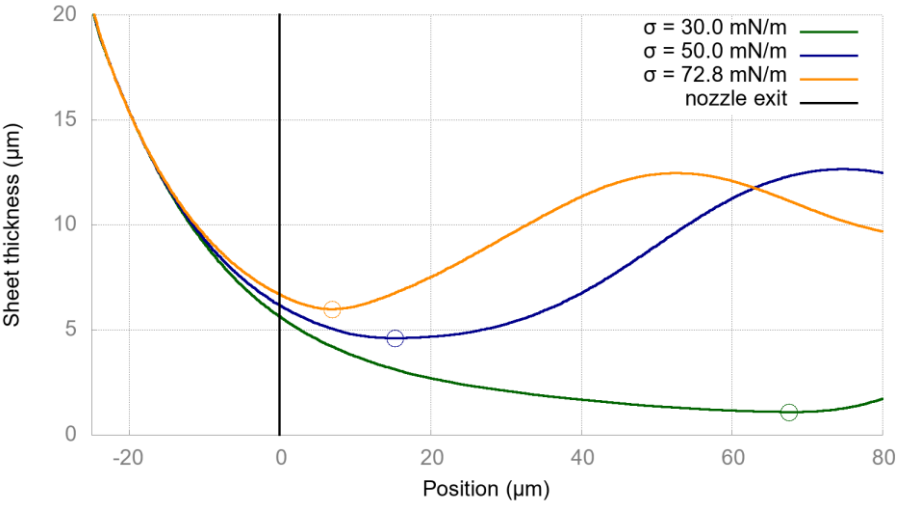

Figure 5: Thickness along the central region of the primary sheet for different surface tensions. The black line denotes the nozzle exit, while the circles represent the minimum achieved sheet thickness.

Table 1: Liquid properties and minimum thickness measurements.

Surface tension coefficient σ $x10^{-3}$ [N/m]	Density ρ [kg/m^3]	Dynamic viscosity μ $x10^{-3}$ [kg/ms]	Primary sheet minimum thickness ± 0.25 [μm]
30	1000	1	1.08
50	1000	1	4.60
72.8	1000	1	5.98
72.8	800	1	5.49
72.8	1200	1	5.98
72.8	1000	0.5	5.73
72.8	1000	1.5	6.23

6 CONCLUSIONS

Results shown here present the effects of liquid properties on the thickness of liquid sheet, produced from the gas focused liquid nozzles. It can be concluded that, though density and viscosity variations do affect the sheet formation, those changes are minimal in comparison to the surface tension impact. This is to be expected since the underlying force that determines the fluid flow under these operating conditions is the surface tension force. Therefore, we conclude that the changes to the surface tension have the largest effect on the sheet formation. Numerical technique used here, especially algebraic volume of fluid, might not be most suitable technique to use for a surface tension driven flow simulations. With such methods one is effectively artificially compressing the interface in order to preserve its sharpness and then calculating the forces exerted on such interface. This might result in deterioration of accuracy and it can be argued that the surface tension driven flow simulations would benefit greatly from geometrical volume of fluid method where precise geometric reconstruction of the interface is performed. This technique is currently not implemented within OpenFOAM. An alternative would be to use the recently developed meshless technique in connection with the phase field formulation [8] to simulate microfluidic liquid sheets. Nevertheless, the results follow a clear trend with varying liquid properties.

ACKNOWLEDGEMENT

Funding for this research is provided by the Centre of Free Electron Laser (CFEL) under project: Innovative methods for imaging with the use of X-ray free electron laser (XFEL) and synchrotron sources: simulation of gas-focused micro-jets, and Slovenian Grant Agency (ARRS) within Program Group P2-0162 and Project J2-7384. The computations were performed on high performance computational resources at Faculty of Mechanical Engineering, University of Ljubljana.

REFERENCES

[1] Warner, J. et al. Gas Dynamic Virtual Nozzle for Generation of Microscopic Droplet Streams. *Journal of Physics D: Applied Physics* (2008) **41(19)**: 195505. http://stacks.iop.org/0022-3727/41/i=19/a=195505.

[2] Gañán-Calvo, A.M. Generation of Steady Liquid Microthreads and Micron-Sized Monodisperse Sprays in Gas Streams. *Physical Review Letters* (1998) **80(2)**: 285–88.

[3] Zahoor, R. et al. Simulation of Liquid Micro-Jet in Free Expanding High-Speed Co-Flowing Gas Streams. *Microfluidics and Nanofluidics* (2018) **22(8)**. http://dx.doi.org/10.1007/s10404-018-2110-0.

[4] Koralek, J.D. et al. Generation and Characterization of Ultrathin Free-Flowing Liquid Sheets. (2018) *Nature Communications* **9(1)**.

[5] Galinis, G. et al. Micrometer-Thickness Liquid Sheet Jets Flowing in Vacuum. *Review of Scientific Instruments* (2017) **88(8)**.

[6] Brackbill, J.U. et al. A Continuum Method for Modeling Surface Tension. *Journal of Computational Physics* (1992) **100(2)**: 335–54.

[7] OpenFOAM. 2010. OpenFOAM Foundation List of Literature 2010. papers2://publication/uuid/BFDC7D14-EB5B-46FF-A6B7-964CD98C7413.

[8] Talat, N. et al. Development of Meshless Phase Field Method for Two-Phase Flow. *International Journal of Multiphase Flow* (2018) **108**: 169–80.